J Breast Cancer. 2021 Oct;24(5):428-442
https://doi.org/10.4048/jbc.2021.24.e42
pISSN 1738-6756·eISSN 2092-9900

Journal of Breast Cancer JBC

Original Article

Long Noncoding-RNA Component of Mitochondrial RNA Processing Endoribonuclease Promotes Carcinogenesis in Triple-Negative Breast Cancer Cells via the Competing Endogenous RNA Mechanism

Received: Feb 1, 2021
Revised: Jun 17, 2021
Accepted: Aug 20, 2021

Correspondence to
Liqiang Qi
Department of Breast Surgical Oncology, Cancer Institute and Cancer Hospital, Chinese Academy of Medical Sciences and Peking Union Medical College, No.17, Panjiayuan Nanli, Chaoyang District, Beijing 100021, China.
E-mail: qiangyuan106586619@163.com

ORCID iDs
Liqiang Qi
https://orcid.org/0000-0003-0085-1078
Bo Sun
https://orcid.org/0000-0003-2527-7156
Beibei Yang
https://orcid.org/0000-0001-7265-7667
Su Lu
https://orcid.org/0000-0002-0311-7955

Funding
This work was supported by Natural Science Foundation of China [81001187].

Conflict of Interest
The authors declare that they have no competing interests.

Liqiang Qi [1], **Bo Sun** [2], **Beibei Yang** [2], **Su Lu** [2]

[1]Department of Breast Surgical Oncology, Cancer Institute and Cancer Hospital, Chinese Academy of Medical Sciences and Peking Union Medical College, Beijing, China
[2]The 2nd Department of Breast Cancer Tianjin Medical University Cancer Institute and Hospital, Tianjin, China

ABSTRACT

Purpose: Triple-negative breast cancer (TNBC) is a subtype of breast cancer. Increasing evidence supports that dysregulation of long noncoding RNAs (lncRNAs) plays a vital role in cancer progression. RNA component of mitochondrial RNA processing endoribonuclease (*RMRP*), a lncRNA, is characterized as a tumor-propeller in some cancers, but its mechanism in TNBC remains poorly understood. This study aimed to determine whether and how *RMRP* functions in TNBC.
Methods: Cell proliferation was determined by cell counting kit-8 (CCK-8) and colony formation assays and cell apoptosis by flow cytometry analysis and terminal deoxynucleotidyl transferase-mediated nick end labeling (TUNEL) assay. Cell migration and invasion were determined by transwell assays. RNA-binding protein immunoprecipitation (RIP), luciferase reporter, and RNA pulldown assays were implemented to assess the interaction of *RMRP* with other molecules in TNBC cells.
Results: *RMRP* expression was elevated in TNBC cells. *RMRP* knockdown repressed cell proliferation, migration, and invasion, but induced apoptosis in TNBC. In addition, *RMRP* was found to target microRNA-766-5p (miR-766-5p) in TNBC cells. Silencing miR-766-5p enhanced cell viability and decreased apoptosis, whereas miR-766-5p overexpression had opposite effects. Furthermore, miR-766-5p was found to bind to yes-associated protein 1 (*YAP1*). Moreover, miR-766-5p inhibition reversed the repressive effect of *RMRP* knockdown on the malignant progression of TNBC.
Conclusion: The present study manifested that *RMRP* promotes the growth, migration, and invasion of TNBC cells via the miR-766-5p/*YAP1* axis. These findings provide novel perspectives for TNBC treatment.

Keywords: Breast neoplasms; MicroRNAs; RNA, untranslated; Triple negative breast neoplasms

Author Contributions

Conceptualization: Sun B; Data curation: Yang B; Formal analysis: Yang B; Investigation: Sun B; Methodology: Sun B; Project administration: Lu S; Resources: Sun B; Software: Lu S; Validation: Qi L; Writing - original draft: Qi L; Writing - review & editing: Qi L.

INTRODUCTION

Breast cancer (BC) is one of the most prevalent malignancies in women. TNBC is the most complex, malignant type of BC characterized by a lack of progesterone receptor, estrogen receptor, and human epidermal growth factor receptor 2 [1]. Currently, clinical treatment approaches for BC patients include surgery, chemotherapy, radiotherapy, or targeted therapy [2], and TNBC patients generally opt chemotherapy owing to a lack of effective targets [3]. Thus, a comprehensive understanding of the underlying molecular mechanisms that induce TNBC pathogenesis, development, and progression is imperative for developing new therapeutic strategies or techniques for TNBC treatment.

Currently, molecular targeting therapy has attracted increasing attention in BC treatment research. Increasing evidence indicated that lncRNAs exert a vital function in the biological processes of BC tumor cell development and progression. For example, BC200 overexpression contributes to luminal BC and TNBC pathogenesis [4]; NEAT1 can promote cell proliferation and metastasis of BC [5]; and MALAT1 represses BC metastasis [6]. LncRNAs are suggested not only as promising prognostic markers in various cancers, but also as a competing endogenous RNA (ceRNA) of microRNA (miRNA) to modulate target gene expression. Notably, the ceRNA regulatory mechanisms of lncRNAs in BC have also been confirmed in previous studies. For instance, HOTAIR affects cell proliferation, metastasis, and apoptosis by regulating miR-20a-5p/HMGA2 axis in BC [7], and lncRNA-CDC6 acts as a ceRNA of miR-215 to target CDC6, promoting BC cell proliferation and metastasis [8].

RMRP is a lncRNA that has been shown to exhibit carcinogenic roles in several human cancers, including hepatocellular carcinoma (HCC) [9], cholangiocarcinoma [10], gastric cancer [11], bladder cancer [12], NSCLC [13], papillary thyroid cancer [14], and neuroblastoma [15]. Nonetheless, the role and mechanism of *RMRP* in TNBC remain to be investigated.

Therefore, this study aimed to determine whether and how *RMRP* functions in TNBC. The expression of *RMRP* in TNBC was measured, and the regulatory roles of *RMRP* in TNBC cell growth, migration, and invasion were investigated through functional experiments. In addition, the target miRNA of *RMRP* and the downstream mRNA of miRNA were explored. Altogether, this study indicated *RMRP* as a novel target for TNBC treatment.

METHODS

Cell lines and cell culture

Human mammary epithelial cell line MCF-10A and TNBC cell lines (MDA-MB-231, MDA-MB-436, and BT-549) were purchased from ATCC (Manassas, USA). As for cell culture, MDA-MB-231 and MDA-MB-436 cells were maintained in Leibovitz's L-15 medium (Sigma-Aldrich, St Louis, USA), BT-549 cells in RPMI-1640 medium (ATCC® 30-2001™; ATCC), and MCF-10A cells in complete growth medium. The abovementioned cell lines were maintained in the corresponding culture medium supplemented with 10% fetal bovine serum (HyClone, Logan, USA) and 1% penicillin-streptomycin (Invitrogen, Carlsbad, USA). All cells were cultured in a 5% CO_2 incubator at 37°C.

https://doi.org/10.4048/jbc.2021.24.e42

Cell transfection and plasmid construction

TNBC cells were seeded into 24-well plates one day before transfection. When cells reached 30% confluence, Lipofectamine™ 2000 (Cat No. 11668-019; Invitrogen) was used to transfect cells based on the supplier's protocols. After 6 hours of transfection, the transfected cells were monitored by the experimenter. The wild-type (WT, with putative miR-766-5p binding sites) or mutant (Mut, with Mut miR-766-5p binding sites) sequence of full-length *RMRP* or *YAP1* 3′-UTR fragments was sub-cloned into pmirGLO vectors (Promega, Madison, USA) to establish *RMRP*/WT or Mut *YAP1*-3′UTR reporter vectors (*YAP1-WT* or *YAP1-Mut*) reporter constructs. Full-length *RMRP* was incorporated into the pcDNA3.1 vector to overexpress *RMRP*; empty pcDNA3.1 was used as a control. In addition, negative control of short hairpin RNA and 3 fragments of interference sequences constructed on the basis of *RMRP* sequence were sub-cloned into the PLRO.1 vector to produce *sh-RMRP* vectors specifically targeting *RMRP* (*sh-RMRP#1*, *sh-RMRP#2*, and *sh-RMRP#3*). The plasmids mentioned above were commercially obtained from GenePharma (Shanghai, China). MiR-766-5p mimics/inhibitors and corresponding NC mimics/inhibitors were procured from RiboBio (Guangzhou, China).

Quantitative polymerase chain reaction (qPCR)

For qPCR analysis, total RNA was extracted using an RNA isolation kit (Thermo Fisher Scientific, Waltham, USA) as per the manufacturer's suggestions. Subsequently, isolated RNAs were reversely transcribed for complementary DNA (cDNA) synthesis using a RevertAid First Strand cDNA Synthesis Kit (Cat#: K1622; Thermo Fisher Scientific) for lncRNA and mRNA and miScript II RT Kit (Cat#: 218160; QIAGEN, Hilden, Germany) for miRNA. qPCR was then conducted using SYBR Green PCR Master Mix (Cat#: 4309155; Applied Biosystems, Foster City, USA) at 95°C for 10 minutes, 95°C for 30 seconds, and 60°C for 30 seconds. Data were examined using the $2^{-\Delta\Delta Ct}$ method. Bio-repeats were performed 3 times for each experiment, and 3 technical replicates were conducted for each bio-repeat. Data are displayed as the mean ± standard deviation. Glyceraldehyde 3-phosphate dehydrogenase (GAPDH) was used as an internal control.

Western blotting

Protein samples were collected from cell lysates using RIPA buffer (Beyotime, Beijing, China) when the cells reached over 80% confluence. Proteins (30 μg) were transferred onto polyvinylidene difluoride (Millipore, Boston, USA) membranes post-separation on 10% sodium dodecyl sulphate-polyacrylamide gel electrophoresis. Afterwards, the membranes were sealed with 5% skim milk in Tris Buffered Saline with Tween 20 (TBST) for 1 hour, followed by incubation with primary antibodies or GAPDH as a loading control at 4°C overnight. Subsequently, the membranes were rinsed 4 times with TBST and then incubated with secondary antibodies (Santa Cruz Biotechnology, Dallas, USA) on a slow shaker for 1 hour, followed by washing with TBST (5 times, 5 min/wash). The membranes were stained with ECL luminous liquid (GE Healthcare, Chicago, USA). The primary antibodies include anti-*YAP1* (ab205270; Abcam, Cambridge, UK), anti-ankyrin repeat domain 1 (ANKRD1, ab272894; Abcam), anti-connective tissue growth factor (CTGF, ab209780; Abcam), and anti-GAPDH (ab8245; Abcam).

CCK-8 assay

The transfected TNBC cells (3×10^4 cells/well) were inoculated into 96-well plates with 100 μL suspension solution in each well and cultivated in an incubator at 37°C. Then, CCK-8 solution (10 μL; Sigma-Aldrich) was added, followed by another 2 hours incubation. A spectrophotometer (Thermo Fisher Scientific) was used to examine the optical density values (450 nm).

https://doi.org/10.4048/jbc.2021.24.e42

Colony formation assay

The indicated transfected TNBC cells (300 cells/well) were inoculated into a 6-well plate, followed by ten-day incubation at 37 °C and 5% CO_2. Subsequent to the incubation, TNBC cells were washed twice using phosphate-buffered saline, fixed using 4% paraformaldehyde, and dyed using crystal violet. Finally, the number of colonies (≥ 50 cells) was counted.

TUNEL

Cells were transfected with the indicated plasmids and subjected to overnight incubation. Transfected cells were then fixed in 4% formaldehyde for 15 minutes, followed by staining with a TUNEL Bright-Red Apoptosis Detection kit (Cat. No. A113; Vazyme, Piscataway, USA). TUNEL-stained cells were observed by fluorescence microscopy (DMI4000B; Leica Microsystems Nussloch GmbH, Nussloch, Germany).

Flow cytometry analysis

TNBC cells were harvested by EDTA-free trypsin and resuspended in binding buffer (500 μL). After staining with Annexin V-FITC (5 μL) and PI (5 μL) (BD Biosciences, San Jose, USA) in the darkness, apoptotic cells were analyzed using a FACSCalibur (BD Biosciences).

Transwell assays

Twenty-four hours post-transfection, TNBC cells were inoculated into the upper compartment of the Transwell system (8 μm pore; Costar Corporation, Washington, D.C., USA) with serum-free Dulbecco's Modified Eagle Medium (DMEM). For the invasion assay, the upper filter was pre-coated with BD Biosciences™ Matrigel. For transwell assays, the lower chamber was added with DMEM with the addition of 20% fetal bovine serum. After a 24 hours incubation, TNBC cells that migrated or invaded the lower chamber were fixed using methanol, stained with 0.2% crystal violet, and photographed using an inverted microscope.

Subcellular fractionation and fluorescence *in situ* hybridization (FISH) assays

For subcellular fractionation assay, nuclear/cytoplasmic RNAs were isolated using nuclear and cytoplasmic extraction reagents (Thermo Fisher Scientific) following the supplier's instructions, followed by qPCR analysis. For FISH assay, after 15 minutes of fixation using 4% paraformaldehyde, cells were permeabilized using TritonX-100 for 15 minutes at 4°C, followed by hybridization with digoxin-labeled *RMRP* (GenePharma). After a brief wash, the fluorescence signal was detected using anti-digoxin antibodies. 4′,6-diamidino-2-phenylindole (Sigma-Aldrich) was for counterstaining. A microscope (DMI4000B; Leica Microsystems GmbH) and the LAS X software were used to acquire images.

RNA pulldown assay

Cells were transfected with *Bio-RMRP-WT* or *Bio-RMRP-Mut*. After 2 PBS washes, the transfected cells were incubated in lysis buffer. After the biotin-labeled RNA complexes were pulled down, qPCR was performed to analyze the expression of potential miRNAs.

Luciferase reporter assay

WT or Mut sequence of full-length *RMRP* or *YAP1* 3′UTR fragments containing predictive binding sites of miR-766-5p were cloned into the pmirGLO vector (Promega). TNBC cells were co-transfected with *RMRP*/*YAP1* reporter vectors, including WT or Mut fragments and miR-766-5p mimics or NC mimics. After 48 hours of transfection, the Dual Luciferase Reporter Assay System (Promega) was used to detect relative luciferase activity as per the supplier's directions. Renilla luciferase was used as an internal control.

https://doi.org/10.4048/jbc.2021.24.e42

RIP

The RIP assay was performed using the Magna RIP® RIP Kit (Millipore). Transfected cells (6×10^7) were lysed in cell lysis buffer. Antibody against immunoglobulin G (Anti-IgG, ab172730; Abcam) and antibody against argonaute 2 (anti-AGO2, ab186733; Abcam) were added to 100 μL cell lysates, while the input group contained 10% cell lysates. Cell lysates were mixed with antibody-bead complexes and incubated overnight at 4°C. qPCR was performed to detect the enrichment of miR-766-5p, *RMRP*, or *YAP1* in IgG- or AGO2-immunoprecipitated complexes. Small nuclear ribonucleoprotein U1 subunit 70 was used as the positive control.

Statistical analysis

Data analyses were conducted using SPSS (version 22.0; IBM, Armonk, USA). The data are displayed as the mean ± standard deviation. Student's *t*-test was adopted for comparison between 2 groups. Comparisons among multiple groups were conducted applying 1-way or 2-way analysis of variance (ANOVA), followed by Dunnett's or Tukey's test. In addition, a *p*-value less than 0.05 indicated statistically significant.

RESULTS

RMRP knockdown hampered cell proliferation, migration, and invasion, but promoted cell apoptosis in TNBC

qPCR analysis showed that the expression of *RMRP* was overtly higher in TNBC cell lines (MDA-MB-231, MDA-MB-436, and BT-549) than in MCF-10A cell line, with MDA-MB-231 and BT-549 cell lines showing the highest *RMRP* expression (**Figure 1A**). To explore the function of *RMRP* in TNBC *in vitro*, we silenced *RMRP* in MDA-MB-231 and BT-549 cells and performed a series of functional experiments. Knockdown of *RMRP* in 2 TNBC cell lines transfected with *sh-RMRP#1/2/3* was verified by qPCR (**Figure 1B**). To evaluate proliferative ability, we performed CCK-8 and colony formation assays and found that downregulation of *RMRP* inhibited the proliferation of TNBC cells (**Figure 1C and D**). TUNEL and flow cytometry assays revealed that *RMRP* knockdown increased cell apoptosis (**Figure 1E and F**, left panel). Additionally, we confirmed that apoptosis of TNBC cells was not altered by *RMRP* knockdown within 24 hours (**Figure 1F**, right panel). Furthermore, transwell assays showed that *RMRP* downregulation suppressed migratory capacity and invasive ability of TNBC cells (**Figure 1G**), indicating that migratory and invasive capacities of TNBC cells were hampered by *RMRP* knockdown and not because of the increase in apoptosis. Additionally, we overexpressed *RMRP* in MCF10A cells using *pcDNA3.1/RMRP* (**Supplementary Figure 1A**). We verified that *RMRP* overexpression triggered cell growth, decreased apoptosis, and promoted migration and invasion of MCF10A cells (**Supplementary Figure 1B-D**). Overall, these results suggested that *RMRP* may have a promoting effect on TNBC cell growth, migration, and invasion and a suppressive effect on cell apoptosis.

MiR-766-5p is the downstream target of *RMRP*

Subsequently, the mechanism of *RMRP* was explored. First, subcellular fractionation and FISH assays were performed to determine the subcellular localization of *RMRP*. The results showed that *RMRP* was predominantly localized in cytoplasm (**Figure 2A and B**). Thus, we speculated that *RMRP* functioned as a ceRNA to interact with miRNAs. To identify *RMRP*-targeted miRNAs, we searched the bioinformatics tool starBase (http://starbase.sysu.edu.cn/), and the following miRNAs were screened: miR-766-5p, miR-1-3p, miR-206, miR-613, miR-580-3p, miR-3142, and miR-1245b-5p (**Figure 2C**). We then verified the binding of *RMRP* with these miRNAs in TNBC cells by RNA pulldown assay and qPCR. The results indicated

https://doi.org/10.4048/jbc.2021.24.e42

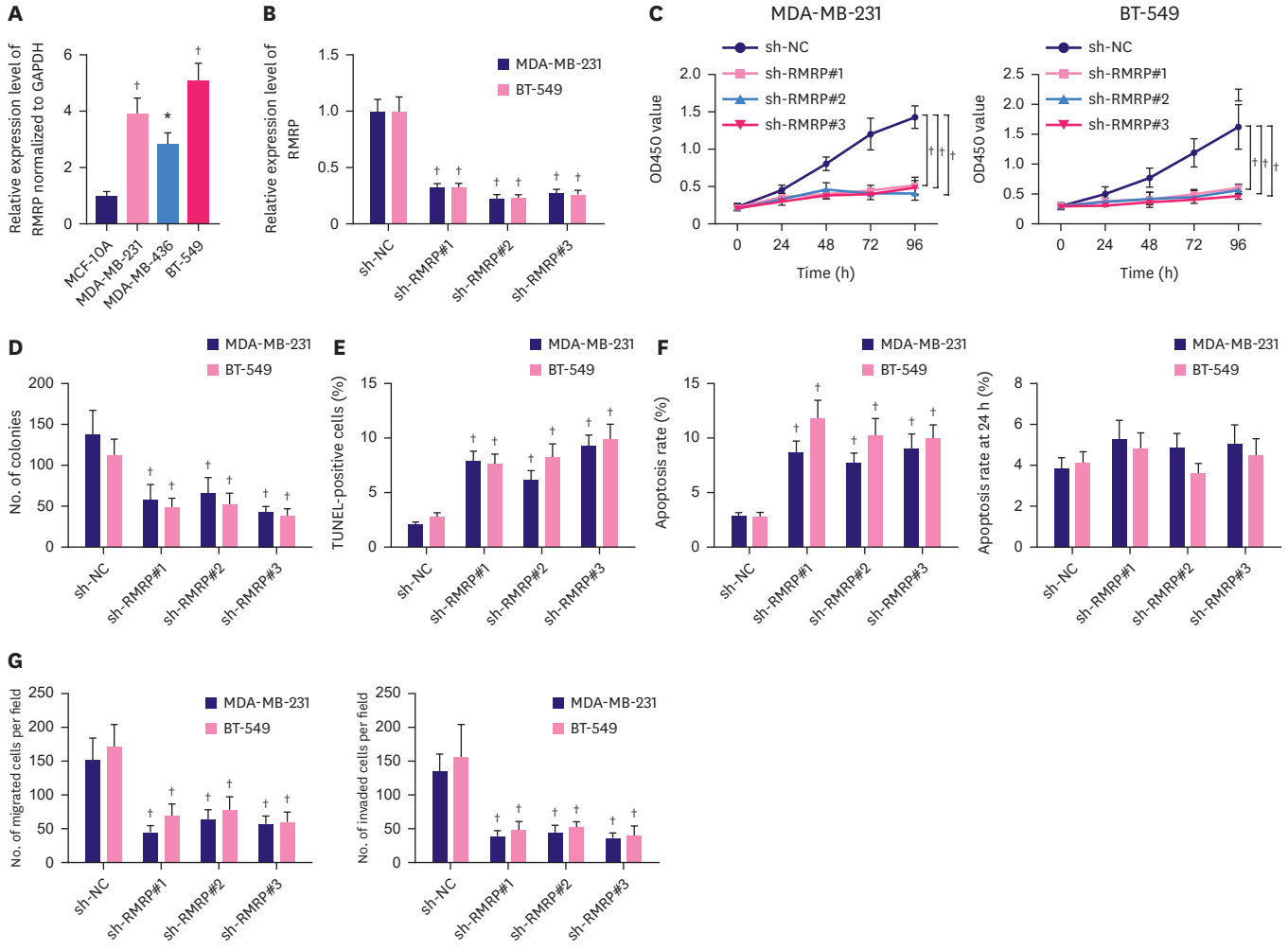

Figure 1. Inhibition of cell proliferation, migration, and invasion and promotion of cell apoptosis in TNBC by *RMRP* knockdown. (A) Relative expression of *RMRP* in TNBC (MDA-MB-231, MDA-MB-436, and BT-549) and MCF-10A cell lines was detected by qPCR. (B) *RMRP* expression was verified by qPCR in TNBC cells transfected with *sh-RMRP#1/2/3* versus sh-NC. (C) CCK-8 assay detected TNBC cell viability following the transfection with *sh-RMRP#1/2/3* versus sh-NC. (D) Quantification of colonies of TNBC cells transfected with *sh-RMRP#1/2/3* versus sh-NC. (E) Ratio of TUNEL-positive TNBC cells in *sh-RMRP#1/2/3* groups versus the sh-NC group. (F) Flow cytometry analysis was implemented to analyze apoptosis of TNBC cells in *sh-RMRP#1/2/3* groups versus the sh-NC group (left panel); flow cytometry analysis was conducted within 24 hours (right panel). (G) The migrated and invaded TNBC cells in *sh-RMRP#1/2/3* groups relative to the sh-NC group in the Transwell system. Data were analyzed with 1-way analysis of variance and Dunnett's test.
GAPDH = glyceraldehyde 3-phosphate dehydrogenase; TNBC = triple-negative breast cancer; sh-NC = negative control of short hairpin RNA; OD = optical density; RMRP = RNA component of mitochondrial RNA processing endoribonuclease; CCK-8 = cell counting kit-8; TUNEL = terminal deoxynucleotidyl transferase-mediated nick end labeling; qPCR = quantitative polymerase chain reaction; N.S. = no significance.
$^{*}p < 0.05$, $^{\dagger}p < 0.01$.

that all 7 miRNAs were significantly enriched in *Bio-RMRP* groups compared with Bio-NC groups, and the fold enrichment of miR-766-5p was the highest among the candidate miRNAs in TNBC cells (**Figure 2D**). Therefore, we speculated that miR-766-5p might be the downstream target of *RMRP*. Furthermore, according to the RIP assay, miR-766-5p and *RMRP* were markedly abundant in the anti-AGO2 group than in the anti-IgG control group (**Figure 2E**). To investigate the miR-766-5p binding sites in *RMRP*, we performed a luciferase reporter assay. We first obtained the predicted miR-766-5p site in *RMRP* from starBase and designed mutated sites with complementary sequences (**Figure 2F**). Results of the luciferase reporter assay showed that the luciferase activity of *RMRP-WT*, but not that of *RMRP-Mut* and pmirGLO vector, was dramatically reduced by miR-766-5p mimics in TNBC cells (**Figure 2G**). Taken together, *RMRP* directly binds to miR-766-5p at the predicted site.

https://doi.org/10.4048/jbc.2021.24.e42

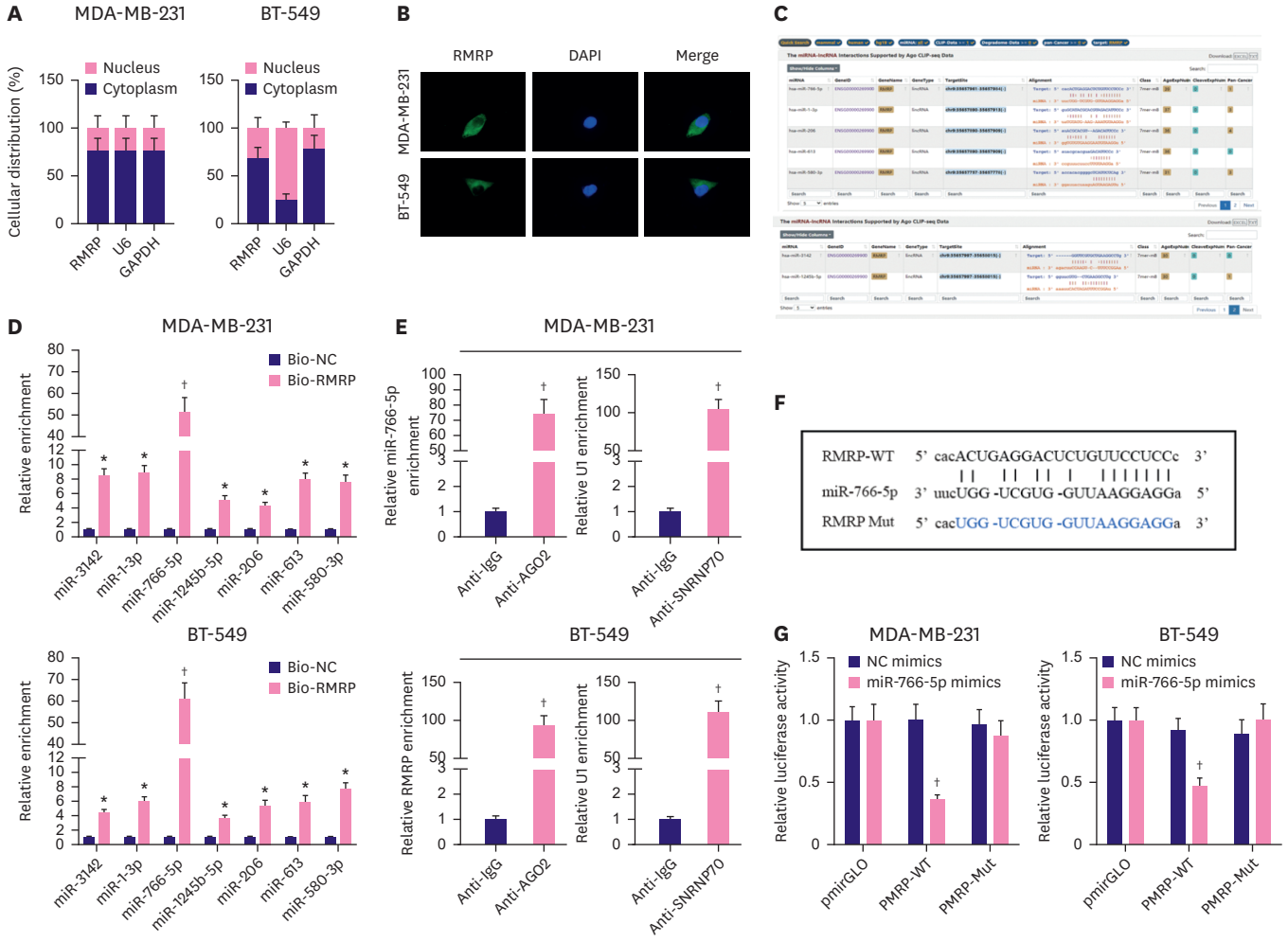

Figure 2. MiR-766-5p as a downstream target of *RMRP*. (A) Subcellular fractionation demonstrated the distribution of *RMRP* in TNBC cells (Student's *t*-test). GAPDH and U6 served as cytoplasmic and nuclear references, respectively. (B) Subcellular localization of *RMRP* in TNBC cells was detected by fluorescence in situ hybridization. Fluorescent stain, ×1,000. (C) Seven potential miRNAs were screened using starBase. (D) RNA pulldown assay was performed followed by qPCR (1-way ANOVA and Tukey's test). *Bio-RMRP* was used to pull down candidate miRNAs. (E) RIP assay was performed with IgG or SNRNP70 as NC or positive control, respectively. Enrichment of miR-766-5p in AGO2 RIP products relative to IgG control was analyzed by qPCR (Student's *t*-test). (F) The sequence of *RMRP-WT* and the sequence of *RMRP-Mut* are shown. (G) The relative luciferase activities in TNBC cells co-transfected with *RMRP-WT* or *RMRP-Mut* and miR-766-5p mimics or NC mimics were detected by luciferase reporter assays (2-way ANOVA and Tukey's test).
RMRP = RNA component of mitochondrial RNA processing endoribonuclease; DAPI = 4′,6-diamidino-2-phenylindole; GAPDH = glyceraldehyde 3-phosphate dehydrogenase; Bio = biotinylated; NC = negative control; Anti-IgG = antibody against immunoglobulin G; Anti-AGO2 = antibody against argonaute 2; Anti-SNRNP70 = antibody against small nuclear ribonucleoprotein U1 subunit 70; WT = wild-type; Mut = mutant; RMRP-WT = RMRP with WT miR-766-5p binding sites; RMRP-Mut = RMRP with Mut miR-766-5p site; TNBC = triple-negative breast cancer; miRNA = microRNA; ANOVA = analysis of variance; RIP = RNA-binding protein immunoprecipitation.
*$p < 0.05$, †$p < 0.01$.

Repression on TNBC cell proliferation, migration, and invasion but promotion on cell apoptosis by miR-766-5p

To further investigate the role of miR-766-5p in TNBC, we knocked down or overexpressed miR-766-5p in TNBC cells. We verified that miR-766-5p inhibitor led to the ablation of miR-766-5p and miR-766-5p mimics led to the upregulation of miR-766-5p in TNBC cells (**Figure 3A**). Proliferation assays revealed that the upregulation of miR-766-5p largely inhibited cell growth, whereas miR-766-5p inhibition had the opposite effect (**Figure 3B-D**). TUNEL and flow cytometry analyses showed that upregulation of miR-766-5p markedly induced cell apoptosis rate, while miR-766-5p silencing reduced the cell apoptosis rate (**Figure 3E and F**). Transwell assays displayed that overexpression of miR-766-5p distinctly lowered the number of migrated and invaded cells,

https://doi.org/10.4048/jbc.2021.24.e42

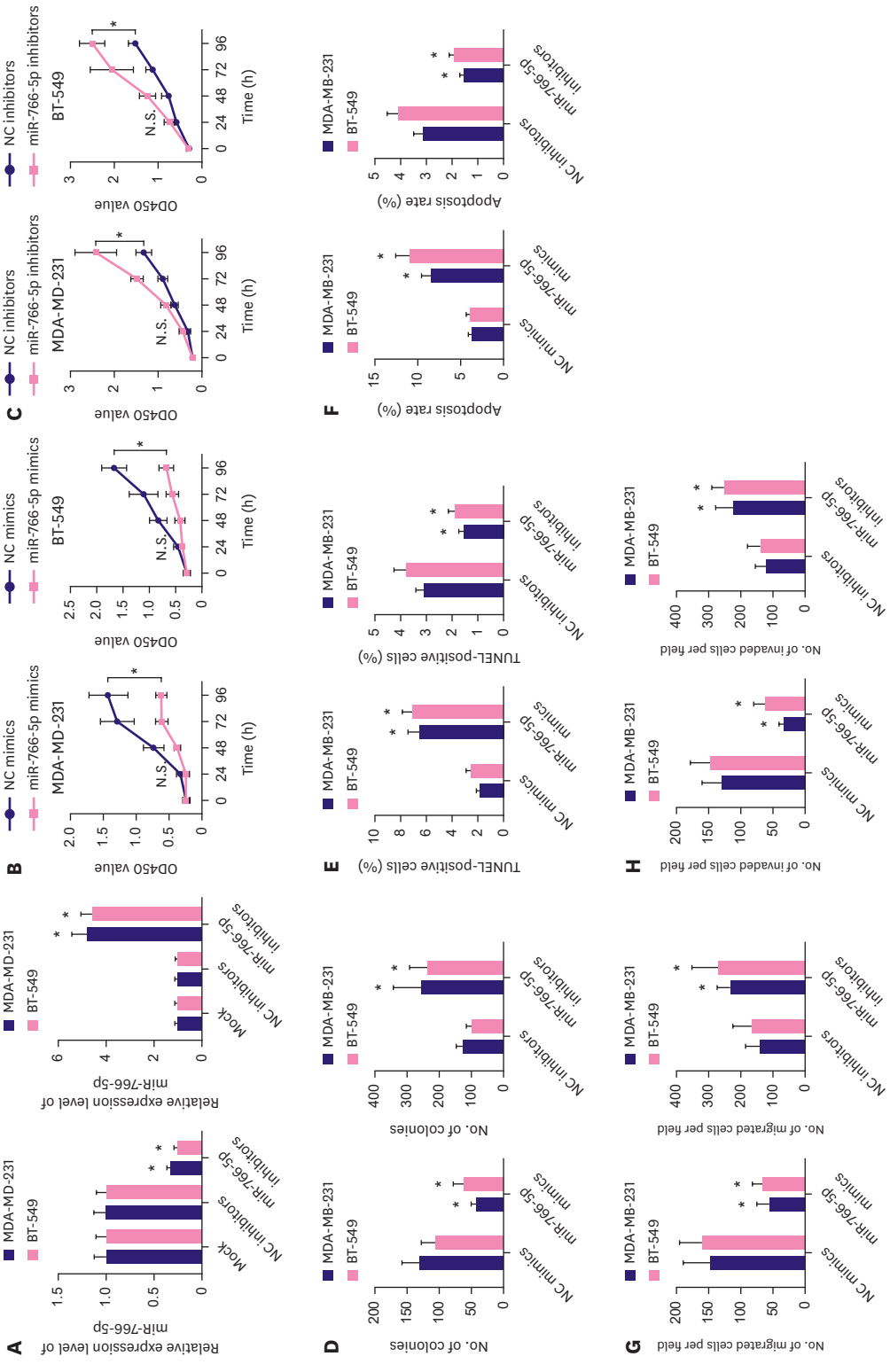

Figure 3. Inhibition of TNBC cell proliferation, migration, and invasion and promotion of cell apoptosis by miR-766-5p. (A) Quantitative polymerase chain reaction data of miR-766-5p in TNBC cells transfected with the miR-766-5p inhibitor versus NC inhibitor or miR-766-5p mimics versus NC mimics (1-way analysis of variance and Tukey's test). (B-D) CCK-8 and colony formation assays were carried out to analyze the effect of miR-766-5p overexpression and knockdown on cell proliferation (Student's *t*-test). (E, F) The apoptosis of TNBC cells was analyzed via TUNEL assay and flow cytometry when miR-766-5p was overexpressed or silenced in TNBC cells (Student's *t*-test). (G, H) Evaluation of TNBC cell migratory and invasive capacities by Transwell and Matrigel assays in the miR-766-5p inhibitor group versus the NC inhibitor group or the miR-766-5p mimics group versus the NC mimics group (Student's *t*-test).
TNBC = triple-negative breast cancer; NC = negative control; OD = optical density; CCK-8 = cell counting kit-8; TUNEL = terminal deoxynucleotidyl transferase-mediated nick end labeling; N.S.: not significant.
*$p < 0.01$.

https://doi.org/10.4048/jbc.2021.24.e42

while low expression of miR-766-5p significantly accelerated cell migration and invasion (**Figure 3G and H**). These results suggest that miR-766-5p suppresses TNBC cell growth, migration, and invasion and enhances cell apoptosis. Additionally, we confirmed that in *RMRP*-overexpressing BT-549 cells, the miR-766-5p inhibitor decreased miR-766-5p levels (**Supplementary Figure 1E**). Moreover, the miR-766-5p inhibitor aggravated cell growth and suppressed apoptosis in *RMRP*-overexpressing BT-549 cells (**Supplementary Figure 1F and G**). Taken together, miR-766-5p represses TNBC cell proliferation, migration, and invasion but promotes cell apoptosis.

RMRP promotes *YAP1* expression via miR-766-5p in TNBC cells

To determine target mRNAs of miR-766-5p, we used starBase, and obtained a large number of potential target mRNAs (CLIP-Data ≥ 3; Pan-Cancer ≥ 4; Program Number ≥ 1; **Figure 4A**). We then conducted a secondary screening on DAVID 6.8 (https://david.ncifcrf.gov/; **Figure 4B**). *YAP1* is one of the key effectors in the Hippo pathway and has been confirmed to be related to TNBC in previous studies [16,17]. Thus, we speculated that *YAP1* is the target downstream of miR-766-5p in TNBC. Herein, we determined whether miR-766-5p affected *YAP1* expression in TNBC cells. qPCR data showed that *YAP1* expression was downregulated by miR-766-5p mimics relative to NC mimic control (**Figure 4C**). Accordingly, western blot analysis demonstrated that the protein expression of *YAP1* was significantly decreased by miR-766-5p mimics (**Figure 4D**). Additionally, effectors downstream of *YAP1*, including CTGF and ANKRD1, were downregulated by miR-766-5p mimics in TNBC cells (**Supplementary Figure 1H and I**). In addition, the RIP assay showed that miR-766-5p, *YAP1*, and *RMRP* were all extremely abundant in the AGO2-binding complexes relative to those in the anti-IgG precipitates (**Figure 4E**). *RMRP* overexpression reduced *YAP1* enrichment in the AGO2 RIP products (**Supplementary Figure 1J**), indicating that overexpression of *RMRP* leads to increased miR-766-5p sponging to prevent *YAP1* from being incorporated into the RNA-induced silencing complex and binding with miR-766-5p mimics. In addition, the miR-766-5p binding site in *YAP1* sequence was identified using starBase (**Figure 4F**). The luciferase activity of TNBC cells transfected with *YAP1-WT* was reduced in the miR-766-5p mimics group relative to the NC mimics group, whereas that of TNBC cells transfected with *YAP1-Mut* was not affected (**Figure 4G**). Overall, these results indicated that *YAP1* is a direct target of miR-766-5p in TNBC. To investigate the regulation of the *RMRP*/miR-766-5p axis on *YAP1*, we performed rescue experiments using TNBC cells and detected mRNA and protein expression of *YAP1* by qPCR and western blot analysis, respectively. It was found that *sh-RMRP#2* caused a decrease on both mRNA and protein expression of *YAP1*, but the miR-766-5p inhibitor reversed the suppressive effect of *RMRP* downregulation on *YAP1* expression (**Figure 4H**). Additionally, miR-766-5p overexpression reversed the promoting effect of *RMRP* overexpression on *YAP1* expression (**Figure 4I**). Collectively, *RMRP* could upregulate *YAP1* expression by competitively sponging miR-766-5p in TNBC cells.

RMRP aggravated proliferative, migratory, invasive capacities and suppressed apoptosis of TNBC cells via miR-766-5p

To determine whether *RMRP* affected the biological process of TNBC cells via miR-766-5p, we performed rescue experiments using BT-549 cells. As expected, the miR-766-5p inhibitor restored the proliferative ability of BT-549 cells repressed by *RMRP* silencing (**Figure 5A and B**). In addition, the cell apoptosis rate increased by *RMRP* knockdown was reversed by the miR-766-5p inhibitor (**Figure 5C and D**). Moreover, miR-766-5p inhibitors restored the number of migrated and invaded cells that were decreased by *sh-RMRP#2* (**Figure 5E**). Altogether, the miR-766-5p inhibitor reversed the suppressive effects of *RMRP* downregulation on the proliferative, migratory, and invasive abilities and the accelerating effect on the apoptotic capacity of TNBC cells. Meanwhile, we confirmed that miR-776-

https://doi.org/10.4048/jbc.2021.24.e42

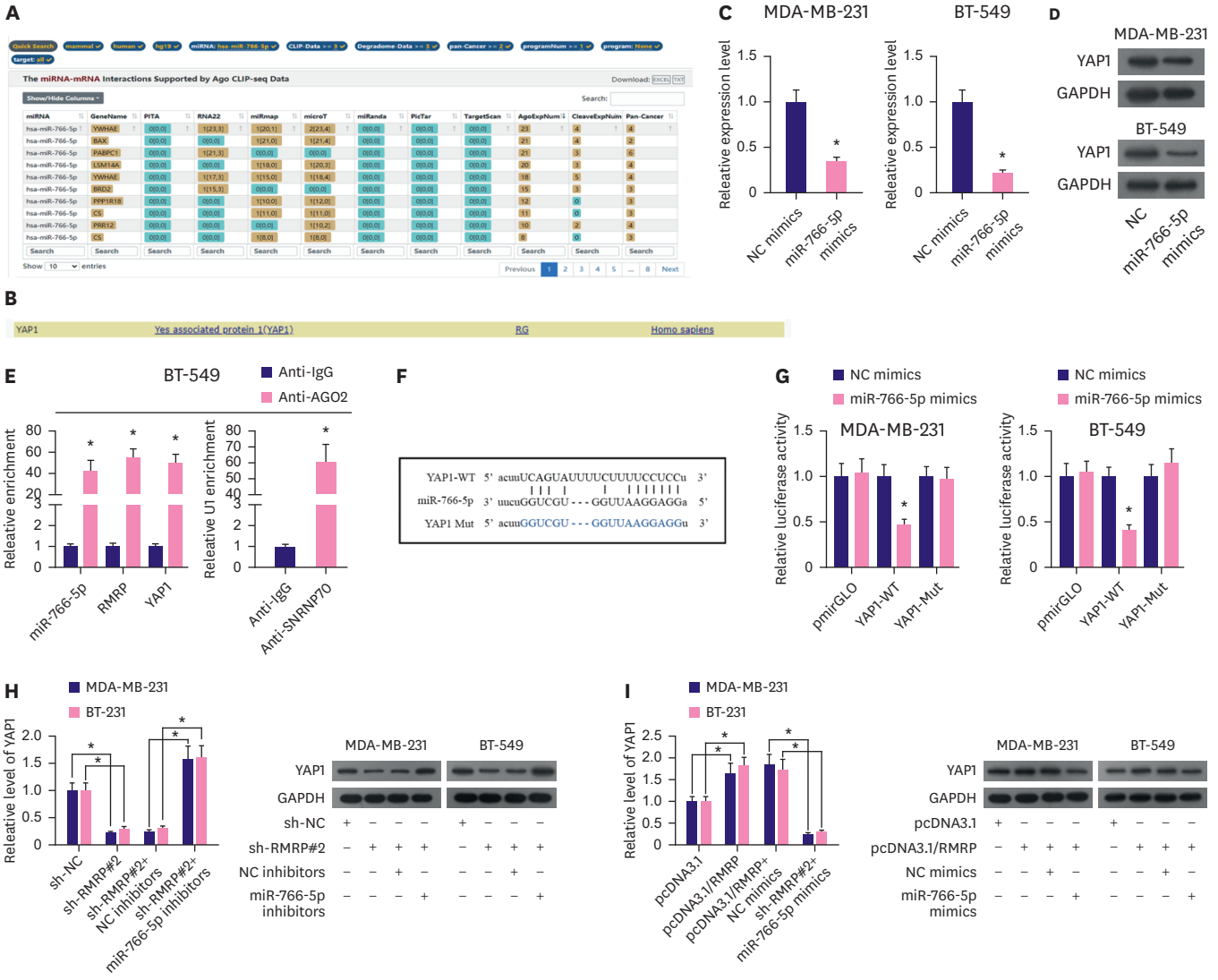

Figure 4. Upregulation of *YAP1* in TNBC cells by *RMRP* via miR-766-5p. (A) Target mRNAs processing binding sites of miR-766-5p were predicted using starBase. (B) *YAP1* was predicted using DAVID 6.8. (C) qPCR was performed to determine the expression of *YAP1* in cells transfected with miR-766-5p mimics versus NC mimics (Student's *t*-test). (D) Western blot analysis was employed to examine the protein expression of *YAP1* in TNBC cells in the miR-766-5p mimics group versus the NC mimics group. (E) RIP assay and qPCR determined the enrichment of *RMRP*, miR-766-5p, and *YAP1* in the binding complex with AGO2 compared to that with IgG (Student's *t*-test). IgG or small nuclear ribonucleoprotein U1 subunit 70 were used as negative control or positive control, respectively. (F) The sequence of binding sites in *YAP1*-3′UTR for miR-766-5p was predicted. (G) *YAP1-WT/Mut* or the empty reporter vector pmirGLO were co-transfected with miR-766-5p mimics or NC mimics into TNBC cells (2-way ANOVA and Tukey's test) and luciferase activities of each group were measured. (H, I) mRNA and protein expression of *YAP1* in the indicated TNBC cells with indicated transfections were analyzed by qPCR (1-way ANOVA and Tukey's test) or western blot analysis.
NC = negative control; YAP1 = yes-associated protein 1; GAPDH = glyceraldehyde 3-phosphate dehydrogenase; Anti-IgG = antibody against immunoglobulin G; Anti-AGO2 = antibody against argonaute 2; RMRP = RNA component of mitochondrial RNA processing endoribonuclease; ANOVA = analysis of variance; qPCR = quantitative polymerase chain reaction; YAP1-WT = WT YAP1-3′UTR reporter vectors; YAP1-Mut = Mut YAP1-3′UTR reporter vectors.
*$p < 0.01$.

5p mimics countervailed the facilitating effect of *RMRP* overexpression on TNBC cell proliferation (**Supplementary Figure 2A and B**). TNBC cell apoptosis was reduced by *RMRP* overexpression and was restored by miR-766-5p mimics (**Supplementary Figure 2C and D**). *RMRP* overexpression strengthened TNBC cell migration and invasion, and this effect was abrogated by miR-766-5p mimics (**Supplementary Figure 2E**). Collectively, *RMRP* was found to drive cell proliferative, migratory, and invasive capacities of TNBC cells and hamper cell apoptosis via miR-766-5p.

https://doi.org/10.4048/jbc.2021.24.e42

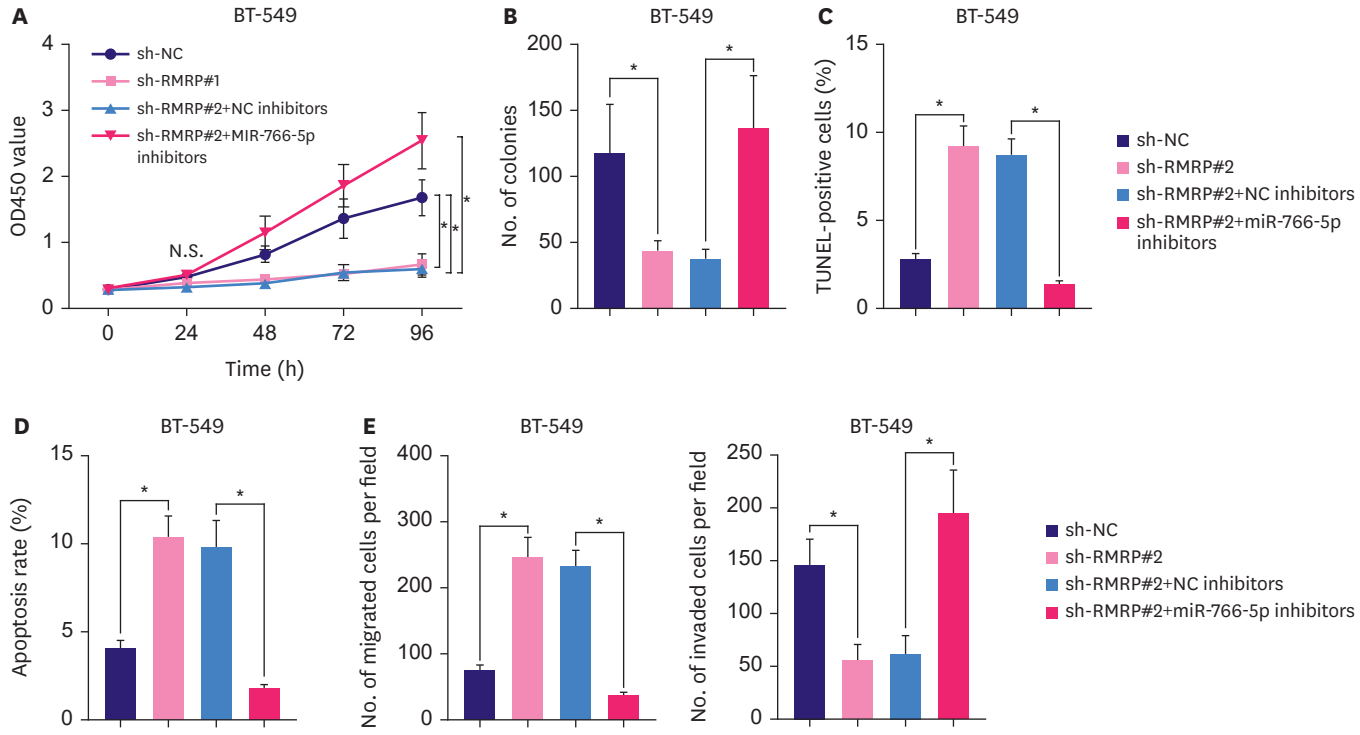

Figure 5. Aggravation of proliferative, migratory, invasive capacities and suppression of apoptosis of triple-negative breast cancer cells by *RMRP* via miR-766-5p. (A) The decreased cell proliferation caused by *sh-RMRP#2* was increased by the miR-766-5p inhibitor. (B) The decreasing number of colonies induced by *RMRP* knockdown was restored by miR-766-5p inhibition. (C) The increasing number of TUNEL-positive cells induced by *RMRP* knockdown markedly decreased following miR-766-5p inhibition. (D) Flow cytometry analysis was conducted to analyze cell apoptosis after the indicated transfection. (E) Transwell assays were performed to analyze cell migration and invasion capacities after *RMRP* knockdown and/or miR-766-5p inhibition.
OD = optical density; sh-NC = negative control of short hairpin RNA; RMRP = RNA component of mitochondrial RNA processing endoribonuclease; NC = negative control; TUNEL = terminal deoxynucleotidyl transferase-mediated nick end labeling; N.S.: not significant.
*$p < 0.01$ was based on 1-way analysis of variance and Tukey's test.

DISCUSSION

As the most aggressive, common and distinct subtype of BC, TNBC has high recurrence rates and dismal clinical prognosis, and the absence of both putative markers and potential therapeutic targets makes it difficult to improve treatment efficacy of TNBC [18]. Thus, further research is needed to identify crucial molecular targets of TNBC.

Recent years have witnessed an increase in lncRNAs proved as potential biomarkers and therapeutic targets for diverse types of cancers, and TNBC is no exception. For example, the expression of TMPO-AS1 is extremely abundant in TNBC cells and its downregulation has shown to inhibit TNBC cell proliferation and migration [19]. Furthermore, AWPPH promotes TNBC cell growth by upregulating FZD7 [20]. Thus, lncRNAs are important molecules that affect TNBC progression. As previously reported, *RMRP* is dysregulated in several types of tumors and has regulatory effects in cancer treatment. For instance, *RMRP* inhibits proliferation, migration, and invasion and promotes apoptosis of HCC cells by targeting miR-766 [21]; additionally, *RMRP* regulates MAPK1 by sponging miR-675 to repress papillary thyroid cancer malignancy [14]. However, *RMRP* also enhances cell proliferation and invasion in NSCLC by targeting miR-1-3p [22], and upregulates c-Myc by sponging miR-34a-5p to enhance cell proliferation and suppress cell apoptosis in multiple myeloma [23]. These studies indicated that the role of *RMRP* varies from one type of cancer to another.

https://doi.org/10.4048/jbc.2021.24.e42

Our study is the first to uncover the mechanism of *RMRP* in TNBC. First, we confirmed that *RMRP* was upregulated in TNBC cell lines, establishing a link with TNBC. Next, functional experiments demonstrated that *RMRP* knockdown negatively regulates cell proliferation, migration, and invasion, but it positively influenced apoptosis of TNBC cells, and *RMRP* overexpression showed opposite effects, indicating that *RMRP* acts as an oncogene in TNBC cells. Additionally, we demonstrated that *RMRP* overexpression could trigger the growth of normal MCF10A cells, indicating that *RMRP* may participate in the initiation of TNBC.

Thereafter, we explored the mechanism of *RMRP* in TNBC cells. Previous studies have largely reported ceRNA mechanisms involving lncRNAs in TNBC. For instance, FAM83H-AS1 enhances TNBC progression via regulating the miR-136-5p/metadherin axis [24], and H19 promotes cell invasion and metastasis through the p53/TNFAIP8 pathway in TNBC [25]. In addition, the role of *RMRP* as ceRNA has been uncovered in other cancers, such as HCC [21] and NSCLC [22]. Our study is the first to confirm that *RMRP* targets miR-766-5p in TNBC cells. Several previous studies have provided *in vitro* data supporting that miR-766-5p is sponged by several lncRNAs and serves as a negative modulator of proliferation and migration in lung cancer [26,27]. Accordingly, our data showed that miR-766-5p negatively influenced TNBC cell growth, migration, and invasion. However, a previous study showed that miR-766-5p cannot affect the growth of MB231 cells *in vivo* but can inhibit sphere formation and invasion *in vitro* [28]. We speculated that this could be because the *in vivo* tumor microenvironment is more complex than the *in vitro* mono-culture of MB231 cells; in the tumor microenvironment, other factors, such as interaction between cells, could affect the function of miR-766-5p in tumorigenesis. Moreover, rescue assays confirmed that miR-766-5p mediated the function of *RMRP* in biological processes of TNBC cells. We first identified *YAP1* as a target of miR-766-5p in TNBC. *YAP1* is an important effector of the Hippo pathway, and it has been characterized as a crucial oncogene in TNBC by former reports. For example, the YAP-ARHGAP42-actin axis contributes to the aggravation of TNBC [29]. YAP nuclear import promotes TNBC metastasis [30]. However, we uncovered the regulation of *YAP1* by *RMRP*/miR-766-5p in TNBC cells. Additionally, we preliminarily confirmed that effectors downstream of *YAP1*, including CTGF and ANKRD1, were also negatively regulated by miR-766-5p in TNBC cells.

However, there are some limitations need to be addressed in further exploration. The current study only focused on *YAP1*, a Hippo signaling pathway-associated effector, which is downstream of the *RMRP*/miR-766-5p axis in TNBC. The mechanism related to the effectors targeted by *YAP1* in TNBC cells will be explored in detail in our future studies. Furthermore, the study lacked *in vivo* experiments to further validate the findings, which will be conducted in our future research.

In a word, the current study is the first to demonstrate that the lncRNA *RMRP* facilitates the malignant progression of TNBC cells, whereas it hinders apoptosis by targeting the miR-766-5p/*YAP1* axis. We also uncovered a marked upregulation of *RMRP* in TNBC cell lines and demonstrated that *RMRP* stimulates cell proliferation, migration, and invasion of TNBC cells. Mechanistically, *RMRP* sponges miR-766-5p to upregulate *YAP1* expression in TNBC cells.

ACKNOWLEDGMENTS

We would like to thank all the people who contributed to this research.

SUPPLEMENTARY MATERIALS

Supplementary Figure 1

Effects of *RMRP* and miR-766-5p on TNBC cell proliferation, migration, invasion, and apoptosis. (A) qPCR detected *RMRP* expression in MCF10A cells transfected with *pcDNA3.1/RMRP* versus pcDNA3.1. (B) CCK-8 assay examined viability of transfected MCF10A cells. (C) Ratio of TUNEL-stained cells in transfected MCF10A cells was evaluated. (D) Number of migrated and invaded transfected MCF10A cells was evaluated. (E) qPCR detected miR-766-5p expression in *RMRP*-overexpressing BT-549 cells in the miR-766-5p inhibitor group versus the NC inhibitor group. (F) CCK-8 assay examined viability of *RMRP*-overexpressing BT-549 cells in the miR-766-5p inhibitor group versus the NC inhibitor group. (G) Ratio of TUNEL-stained *RMRP*-overexpressing BT-549 cells in the miR-766-5p inhibitor group versus the NC inhibitor group was evaluated. (H, I) qPCR and western blot detected the expression of CTGF and ANKRD1 in TNBC cells in the miR-766-5p mimics group versus the NC mimics group. (J) RNA binding protein immunoprecipitation and qPCR detected the enrichment of *YAP1* in the binding complex with AGO2 relative to IgG in BT-549 cells in the *pcDNA3.1/RMRP* group versus the pcDNA3.1 group.

Click here to view

Supplementary Figure 2

Regulation of *RMRP* on proliferative, migratory, invasive capacities, and apoptosis of TNBC cells via miR-766-5p. (A) BT-549 cells were transfected with pcDNA3.1, *pcDNA3.1/RMRP*, *pcDNA3.1/RMRP*+NC mimics, or *pcDNA3.1/RMRP*+ miR-766-5p mimics. CCK-8 assay detected the viability of BT-549 cells in each group. (B) The number of colonies of BT-549 cells in each group was evaluated. (C) Ratio of TUNEL-stained BT-549 cells in each group was evaluated. (D) Ratio of apoptotic BT-549 cells in each group was evaluated by flow cytometry analysis. (E) The number of migrated and invaded BT-549 cells in each group in a Transwell system was evaluated.

Click here to view

REFERENCES

1. Tang L, Chen Y, Tang X, Wei D, Xu X, Yan F. Long noncoding RNA *DCST1-AS1* promotes cell proliferation and metastasis in triple-negative breast cancer by forming a positive regulatory loop with miR-873-5p and MYC. J Cancer 2020;11:311-23.
PUBMED | CROSSREF
2. Peart O. Breast intervention and breast cancer treatment options. Radiol Technol 2015;86:535M-558M.
PUBMED
3. Hwang SY, Park S, Kwon Y. Recent therapeutic trends and promising targets in triple negative breast cancer. Pharmacol Ther 2019;199:30-57.
PUBMED | CROSSREF
4. Barton M, Santucci-Pereira J, Vaccaro OG, Nguyen T, Su Y, Russo J. BC200 overexpression contributes to luminal and triple negative breast cancer pathogenesis. BMC Cancer 2019;19:994.
PUBMED | CROSSREF
5. Zhang M, Wu WB, Wang ZW, Wang XH. lncRNA NEAT1 is closely related with progression of breast cancer via promoting proliferation and EMT. Eur Rev Med Pharmacol Sci 2017;21:1020-6.
PUBMED
6. Kim J, Piao HL, Kim BJ, Yao F, Han Z, Wang Y, et al. Long noncoding RNA MALAT1 suppresses breast cancer metastasis. Nat Genet 2018;50:1705-15.
PUBMED | CROSSREF

7. Zhao W, Geng D, Li S, Chen Z, Sun M. LncRNA HOTAIR influences cell growth, migration, invasion, and apoptosis via the miR-20a-5p/HMGA2 axis in breast cancer. Cancer Med 2018;7:842-55.
PUBMED | CROSSREF
8. Kong X, Duan Y, Sang Y, Li Y, Zhang H, Liang Y, et al. LncRNA-CDC6 promotes breast cancer progression and function as ceRNA to target CDC6 by sponging microRNA-215. J Cell Physiol 2019;234:9105-17.
PUBMED | CROSSREF
9. Zhou N, He Z, Tang H, Jiang B, Cheng W. LncRNA RMRP/miR-613 axis is associated with poor prognosis and enhances the tumorigenesis of hepatocellular carcinoma by impacting oncogenic phenotypes. Am J Transl Res 2019;11:2801-15.
PUBMED
10. Tang L, Wang Y, Wang H, Xu B, Ji H, Xu G, et al. Long noncoding-RNA component of mitochondrial RNA processing endoribonuclease is involved in the progression of cholangiocarcinoma by regulating microRNA-217. Cancer Sci 2019;110:2166-79.
PUBMED | CROSSREF
11. Shao Y, Ye M, Li Q, Sun W, Ye G, Zhang X, et al. LncRNA-RMRP promotes carcinogenesis by acting as a miR-206 sponge and is used as a novel biomarker for gastric cancer. Oncotarget 2016;7:37812-24.
PUBMED | CROSSREF
12. Cao HL, Liu ZJ, Huang PL, Yue YL, Xi JN. lncRNA-RMRP promotes proliferation, migration and invasion of bladder cancer via miR-206. Eur Rev Med Pharmacol Sci 2019;23:1012-21.
PUBMED | CROSSREF
13. Yang M, Ke H, Zhou W. LncRNA RMRP promotes cell proliferation and invasion through miR-613/NFAT5 axis in non-small cell lung cancer. Onco Targets Ther 2020;13:8941-50.
PUBMED | CROSSREF
14. Wang J, Xiao T, Zhao M. MicroRNA-675 directly targets MAPK1 to suppress the oncogenicity of papillary thyroid cancer and is sponged by long non-coding RNA RMRP. Onco Targets Ther 2019;12:7307-21.
PUBMED | CROSSREF
15. Pan J, Zhang D, Zhang J, Qin P, Wang J. LncRNA RMRP silence curbs neonatal neuroblastoma progression by regulating microRNA-206/tachykinin-1 receptor axis via inactivating extracellular signal-regulated kinases. Cancer Biol Ther 2019;20:653-65.
PUBMED | CROSSREF
16. Andrade D, Mehta M, Griffith J, Panneerselvam J, Srivastava A, Kim TD, et al. YAP1 inhibition radiosensitizes triple negative breast cancer cells by targeting the DNA damage response and cell survival pathways. Oncotarget 2017;8:98495-508.
PUBMED | CROSSREF
17. Gan L, Camarena V, Mustafi S, Wang G, Vitamin C. Vitamin C inhibits triple-negative breast cancer metastasis by affecting the expression of YAP1 and synaptopodin 2. Nutrients 2019;11:2997.
PUBMED | CROSSREF
18. Ding L, Gu H, Xiong X, Ao H, Cao J, Lin W, et al. MicroRNAs involved in carcinogenesis, prognosis, therapeutic resistance and applications in human triple-negative breast cancer. Cells 2019;8:1492.
PUBMED | CROSSREF
19. Mitobe Y, Ikeda K, Sato W, Kodama Y, Naito M, Gotoh N, et al. Proliferation-associated long noncoding RNA, TMPO-AS1, is a potential therapeutic target for triple-negative breast cancer. Cancer Sci 2020;111:2440-50.
PUBMED | CROSSREF
20. Wang K, Li X, Song C, Li M. LncRNA AWPPH promotes the growth of triple-negative breast cancer by up-regulating frizzled homolog 7 (FZD7). Biosci Rep 2018;38:BSR20181223.
PUBMED | CROSSREF
21. Shao C, Liu G, Zhang X, Li A, Guo X. Long noncoding RNA RMRP suppresses the tumorigenesis of hepatocellular carcinoma through targeting microRNA-766. Onco Targets Ther 2020;13:3013-24.
PUBMED | CROSSREF
22. Wang Y, Luo X, Liu Y, Han G, Sun D. Long noncoding RNA RMRP promotes proliferation and invasion via targeting miR-1-3p in non-small-cell lung cancer. J Cell Biochem 2019;120:15170-81.
PUBMED | CROSSREF
23. Xiao X, Gu Y, Wang G, Chen S. c-Myc, RMRP, and miR-34a-5p form a positive-feedback loop to regulate cell proliferation and apoptosis in multiple myeloma. Int J Biol Macromol 2019;122:526-37.
PUBMED | CROSSREF
24. Han C, Fu Y, Zeng N, Yin J, Li Q. LncRNA FAM83H-AS1 promotes triple-negative breast cancer progression by regulating the miR-136-5p/metadherin axis. Aging (Albany NY) 2020;12:3594-616.
PUBMED | CROSSREF

25. Li Y, Ma HY, Hu XW, Qu YY, Wen X, Zhang Y, et al. LncRNA H19 promotes triple-negative breast cancer cells invasion and metastasis through the p53/TNFAIP8 pathway. Cancer Cell Int 2020;20:200.
PUBMED | CROSSREF

26. Bai Y, Zhang G, Cheng R, Yang R, Chu H. CASC15 contributes to proliferation and invasion through regulating miR-766-5p/ KLK12 axis in lung cancer. Cell Cycle 2019;18:2323-31.
PUBMED | CROSSREF

27. Wang M, Liao Q, Zou P. PRKCZ-AS1 promotes the tumorigenesis of lung adenocarcinoma via sponging miR-766-5p to modulate MAPK1. Cancer Biol Ther 2020;21:364-71.
PUBMED | CROSSREF

28. Oh K, Lee DS. *In vivo* validation of metastasis-regulating microRNA-766 in human triple-negative breast cancer cells. Lab Anim Res 2017;33:256-63.
PUBMED | CROSSREF

29. Jiang K, Liu P, Xu H, Liang D, Fang K, Du S, et al. SASH1 suppresses triple-negative breast cancer cell invasion through YAP-ARHGAP42-actin axis. Oncogene 2020;39:5015-30.
PUBMED | CROSSREF

30. Chen W, Bai Y, Patel C, Geng F. Autophagy promotes triple negative breast cancer metastasis via YAP nuclear localization. Biochem Biophys Res Commun 2019;520:263-8.
PUBMED | CROSSREF